is observed in this case. This result distinguishes $E2$ from $M1$ three-wave mixing, in which generation occurs when $\vec{H}$, $\vec{E}_1$, and $\vec{E}_2$ are parallel.[3]

(b) $\vec{H}+H\hat{x}$, $\vec{E}_2$ along $\hat{y}$. Only the H-dependent term contributes; hence, $I \propto n^2 l^2 H^2 |E_1|^2 |E_2|^2 \propto nH^2 |E_1|^2 \times |E_2|^2$, as observed (Figs. 1 and 2).

(c) $\vec{H}=\pm H\hat{y}$, $\vec{E}_2$ perpendicular to $\hat{y}$. From Eqs. (2), (4), and (5) we obtain

$$I \propto n^2 l^2 |E_1|^2 |E_2|^2 [\theta^2 \int |\mu_0(\omega)|^2 |f(\omega)|^2 d\omega \mp 2H\theta \int \mu_0(\mu_1 - \mu_2) |f(\omega)|^2 d\omega + H^2 \int |\mu_1 - \mu_2|^2 |f(\omega)|^2 d\omega],$$

which explains the shape of Fig. 3 and the simplicity of the combinations plotted in Fig. 4. The minimum of Fig. 3 ($\theta = 35$ mrad) occurs at $H = 25$ G which, for $\Gamma \cong 3\times 10^{10}$ sec^{-1},[2] is in reasonable agreement with the expected value $\cong \theta\hbar\Gamma/\mu_B \cong 100$ G.

(d) $\vec{H}=\pm H\hat{x}$, $\vec{E}_2$ perpendicular to $\hat{y}$. Since $\vec{E}_0$ is perpendicular to $\vec{E}'$, the intensities of the noncollinear and magnetically induced signals add, and $I(H) - I(H=0) \propto H^2$. This prediction was verified in our experiment.

To summarize, we have observed the effect of a magnetic field on SFG in atomic Na vapor. Depending on experimental conditions, the unperturbed SFG can be either enhanced or degraded. All observations are in agreement with theory. Similar effects should be observable in DFG.

*This work was supported by the Joint Services Electronics Program (U. S. Army, U. S. Navy, and U. S. Air Force) under contract No. DAAB07-74-C-0341.

[1]P. A. Franken, A. E. Hill, C. W. Peters, and G. Weinreich, Phys. Rev. Lett. 7, 118 (1961); J. Armstrong, N. Bloembergen, J. Ducuing, and P. S. Pershan, Phys. Rev. 127, 1918 (1962); G. D. Boyd, A. Ashkin, J. M. Dziedzic, and D. A. Kleinman, Phys. Rev. 137, A1305 (1964); M. D. Martin and E. L. Thomas, IEEE J. Quant. Electron. 2, 196 (1966); Van Tran Nguyen and T. J. Bridges, Phys. Rev. Lett. 29, 359 (1972); Terrence L. Brown and P. A. Wolff, Phys. Rev. Lett. 29, 362 (1972); R. G. Smith, in *Laser Handbook*, edited by F. T. Arecchi and E. O. Schultz-Dubois (North-Holland, Amsterdam, 1972), and references therein. See also P. S. Pershan, Phys. Rev. 130, 919 (1963); T. Hänsch and P. Toschak, Z. Phys. 236, 373 (1970).

[2]D. S. Bethune, R. W. Smith, and Y. R. Shen, Phys. Rev. Lett. 37, 431 (1976).

[3]A. Flusberg, T. Mossberg, and S. R. Hartmann, Phys. Rev. Lett. 38, 59 (1977).

[4]A. Flusberg, T. Mossberg, and S. R. Hartmann, Phys. Rev. A 14, 2146 (1976), Appendix A.

[5]Pershan, Ref. 1; Hänsch and Toschak, Ref. 1.

[6]A. Flusberg, T. Mossberg, and S. R. Hartmann, to be published.

[7]In the limit $\Omega_{bb'} \to 0$, the ratio $[g(\omega - \Omega_{ba}) - g(\omega - \Omega_{b'a})]\Omega_{bb'}^{-1} \to dg/d\omega$ is well defined.

[8]Equivalently, the effect of the magnetic field in producing three-wave mixing is of order $(\vec{M}\cdot\vec{H})/\hbar\Gamma$, where Γ is the Doppler width if depolarizing collisions may be neglected. This result is derived in Ref. 6. We note that in Ref. 3 it was stated that for DFG on the $T1$ $6^2P_{1/2}$-$6^2P_{3/2}$ transition, the effect of $\vec{H}$ is of order $(\vec{M}\cdot\vec{H})/\hbar\Delta\omega$, where $\Delta\omega/2\pi$ is the $6^2P_{3/2}$-state hyperfine splitting (520 MHz). This statement is misleading; DFG will occur via magnetic mixing of *Zeeman* levels even in the absence of hyperfine splitting. The effect of $\vec{H}$ is always of the order of $(\vec{M}\cdot\vec{H})/\hbar\Gamma$. The estimate of Ref. 3 is valid, however, since for the transition in question, $\Delta\omega \cong$ the Doppler width Γ.

Thermal-Force Terms and Self-Generated Magnetic Fields in Laser-Produced Plasmas

D. G. Colombant and N. K. Winsor
Naval Research Laboratory, Washington, D. C. 20375
(Received 15 September 1976)

The several magnetic-source terms affecting laser-produced plasmas are presented and their importance discussed. The thermal force is shown to greatly modify the magnetic-field distribution in numerical simulations. Experimental implications are also discussed.

In 1971, self-generated magnetic fields were proposed as an explanation of some physical phenomena in laser-produced plasmas.[1] Since that time, their presence has been confirmed experimentally,[2,3] and a number of theoretical reasons have been given why they may be expected to have an important effect on the plasma dynamics.[4-7] We present here analysis of these effects, and draw attention to the features of the magnetic-field source terms which may assist further experimental studies.

In these studies, we use a computational model which has been described in detail elsewhere.[8] Using a simplified magnetic-source term, it has

shown the crucial importance of magnetic fields in the interpretation of continuum x-ray spectra from targets of high-intensity (10^{16} W/cm^2) neodymium lasers.[9] In this Letter we show how that result is altered by the complete form of the magnetic-source terms, and show why an experimental measurement of the magnetic field should be made late in the laser pulse and well outside the critical surface.

The magnetic-source term for the present work is obtained from the generalized Ohm's Law as derived by Braginskii.[10] Taking its curl yields

$$\frac{\partial \vec{B}}{\partial t} = \nabla \times \left[\vec{V} \times \vec{B} - \frac{c^2}{4\pi} \vec{\vec{\eta}} \cdot (\nabla \times \vec{B}) \right] - \frac{ck}{eN_e} \nabla N_e \times \nabla T_e - \frac{c}{4\pi e} \nabla \times \left[\frac{1}{N_e} (\nabla \times \vec{B}) \times \vec{B} \right] - \frac{c}{e} \nabla \times (\beta \nabla T_e - \alpha \hat{b} \times \nabla T_e), \quad (1)$$

where $\vec{V}$ is the fluid velocity, $\vec{\vec{\eta}}$ the resistivity tensor, N_e the electron density, T_e the electron temperature, and α and β are coefficients depending on $\omega_{ce}\tau_{ei}$. [Comparison of Eq. (4.31) of Ref. 10 with our Eq. (1) defines our α and β.]

The central point of this Letter is that all of the terms in Eq. (1) are of comparable magnitude during simulations of laser-plasma experiments. All must be retained to assess quantitatively the magnetic-field effects. A short analysis of the terms in Eq. (1) will aid the interpretation of the results to be presented below.

The first set of square brackets in Eq. (1) contains the convection (origin of the "frozen-in" law) and diffusion terms; they are the classical magnetohydrodynamic terms, and give the dominant effects of plasma motion and finite conductivity on the magnetic field. Strictly speaking, they are not source terms, since they only transport magnetic field from one place to another, and vanish if $B = 0$. The second term (the "basic" one) in Eq. (1) is due to nonparallel density and temperature gradients, and is the only one used by most authors; it originates from the electron pressure term,

$$(ck/eN_e)\nabla N_e \times \nabla T_e = (c/e)\nabla \times [N_e^{-1} \nabla N_e k T_e], \quad (2)$$

and is largest near the edge of the laser focal spot, where the radial temperature gradient is largest. The third term in Eq. (1) is composed of a curvature term and a magnetic-pressure term and we have

$$(c/4\pi e)\nabla \times [N_e^{-1}(\nabla \times \vec{B}) \times \vec{B}] = (c/e)\nabla \times [(4\pi N_e)^{-1}(\vec{B} \cdot \nabla \vec{B} - \tfrac{1}{2}\nabla B^2)]. \quad (3)$$

The magnetic-pressure term is normally small since the magnetic pressure is seldom more than a few percent of the plasma pressure. The last term in Eq. (1) is the thermal-force term; it is due to the unbalance of the friction force on electrons in the presence of a thermal gradient. It would appear from Eq. (1) that this last term [like the second term as shown in Eq. (2)] will create magnetic field where none was present. However, this is not the case—when $B = 0$, $\alpha = 0$ and $\beta \propto N_e$, so that the curl vanishes. Thus the second term [as shown in Eq. (2)] provides the initial "seed" field; and the other terms come into play as $\omega_e\tau_e$ becomes of order 1.

The reason why all the terms must be kept is that, with the basic source of Eq. (2) alone [i.e., the second term in Eq. (1)], one expects $\omega_e\tau_e \gg 1$ in the region where most of the laser energy is being deposited during most of the deposition. Thus one might expect all the terms to contribute to the evolution of the magnetic field.

Figure 1 presents the magnetic-field contours early and late in an experiment described in detail in Ref. 9. These results use the complete

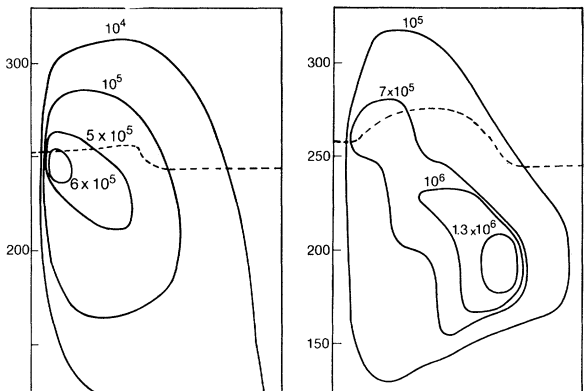

FIG. 1. Magnetic-field (in gauss) contours computed using the complete model, at (a) 22 psec and (b) 62 psec. Experiment is with a 1-J Nd-laser pulse, 12-μm-radius focal spot, and a 21-psec FWHM pulse incident on a CH_2 target. The laser pulse is incident from the bottom of the page, with the laser centerline on the left edge of each picture. The spatial scale is in microns; and the broken line represents the critical surface.

magnetic-source model of Eq. (1), and represent our best estimate of the resulting fields. The computational model used is as described in Ref. 8, except that all the laser energy which reaches the critical depth is deposited there. The neodymium-laser pulse contains 1 J, with Gaussian space and time distributions, 12-μm-radius, and 21-psec full width at half-maximum (FWHM) intensity. The target is planar solid CH_2 with an exponential density tail having an e-folding length (which is a computational artifice whose effect will be discussed below) of 27 μm in front of the target.

Figure 2 presents computational results for the same experiment but with the thermal-force term absent from the model.[9] The numerical parameters were the same as those used for Fig. 1; in particular, the grid size was the same (12 μm in both directions). The differences between results of Figs. 1 and 2 then indicate the sensitivity of the results to the thermal-force term. Comparing these cases, we find that the presence of the thermal-force term has several important effects: (a) It reduces the magnitude of the magnitude of the maximum B. (b) The maximum is reached much later in time—70 psec after the peak of the laser pulse in this case. (c) It is reached at much larger radius (100 μm versus 12 μm). (d) It is much further outside the critical surface (100 μm versus 20 μm). (e) At all times, there is less detailed structure in the contours; the source terms exhibit fewer changes of sign. Therefore, the thermal-force term clearly alters both where one would expect to find the magnetic field and what it does to the plasma.

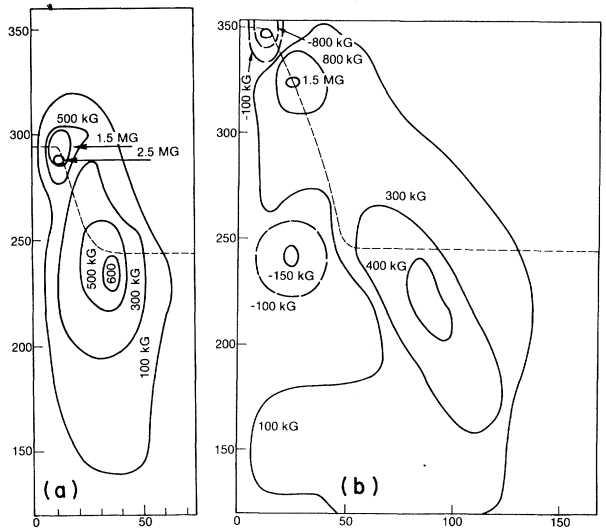

FIG. 2. Same computation as in Fig. 1, but without thermal-force terms, at (a) 18 psec and (b) 89 psec. Note irregular structure, with megagauss fields at much smaller radius (closer to left edge of pictures).

In view of these substantial changes, and in particular item (e) above, it is appropriate to decompose the complete magnetic-source term, and see whether a new term is dominant. The spatial region just outside the laser focus, where the incomplete source terms produce field reversal, is of particular interest. The terms of Eq. (3) [i.e., the third term in Eq. (1)] are not important, as remarked above. The second and fourth terms of Eq. (1) will be decomposed as follows:

$$\frac{\partial B}{\partial t} = \cdots - \frac{ck}{eN_e}\left(\frac{\partial N_e}{\partial z}\frac{\partial T_e}{\partial r} - \frac{\partial N_e}{\partial r}\frac{\partial T_e}{\partial z}\right) + \cdots + \frac{c}{e}\left[\frac{\partial \beta}{\partial r}\frac{\partial T_e}{\partial z} - \frac{\partial \beta}{\partial z}\frac{\partial T_e}{\partial r} + \frac{\partial}{\partial z}\left(\alpha\frac{\partial T_e}{\partial z}\right) + \frac{\partial}{\partial r}\left(\alpha\frac{\partial T_e}{\partial r}\right)\right]. \quad (4)$$

These terms are labeled in the order of their appearance in Eq. (4) and depicted in Fig. 3. Note that, on the left-hand side of the figure, where the basic-source terms (1) and (2) [derived from the second term in Eq. (1)] would be producing field reversal, terms (3) and (5) (which are proportional to $\partial T_e/\partial z$) are dominant.

Physically, the dynamics may be described as follows. At initiation of laser absorption, the basic term (1) brings the magnetic field to $\omega_e\tau_e \gg 1$ near the critical surface in a few picoseconds. As the target responds to the laser-energy deposition, flux limitation (magnetic or otherwise) increases $\partial T_e/\partial z$, and hydrodynamic motion increases $\partial N_e/\partial z$. In the basic case, the sign of term (2) would tend to reverse the sign of the source term. Figure 3 shows that terms (3) and (5) are dominant in the complete source term, and maintain the original sign of the source term.

It appears to the authors that the fine structure evidenced in Fig. 2 is an indication that the basic model is incomplete, and the apparent turbulence is driven by unbalanced terms resulting from the absence of some essential physics. The smooth magnetic distributions of Fig. 1, resulting as they do from the complex structure of the source terms evidenced in Fig. 3, demonstrate that these source terms are cooperating in an essential way with the convective and diffusive terms of the complete magnetic-field equation [Eq. (1)].

We have remarked above that, for computation-

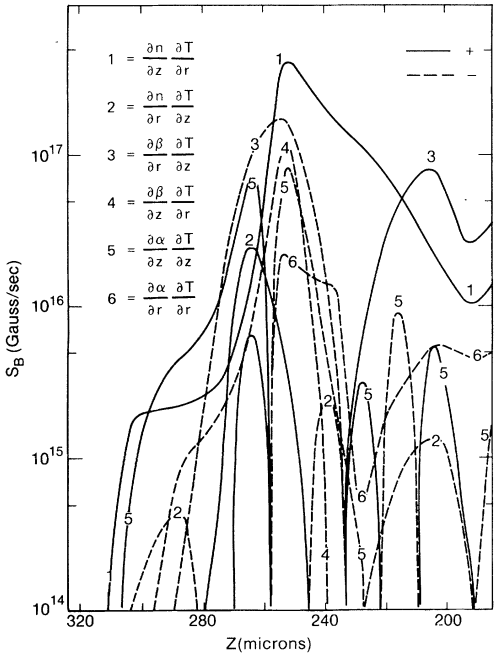

FIG. 3. Individual contributions [(Eq. (14)] to the complete magnetic-source model for case of Fig. 1(a). The horizontal scale of this figure corresponds to the vertical scale of Fig. 1(a); and the depicted source terms are at a constant radius of 12 μm.

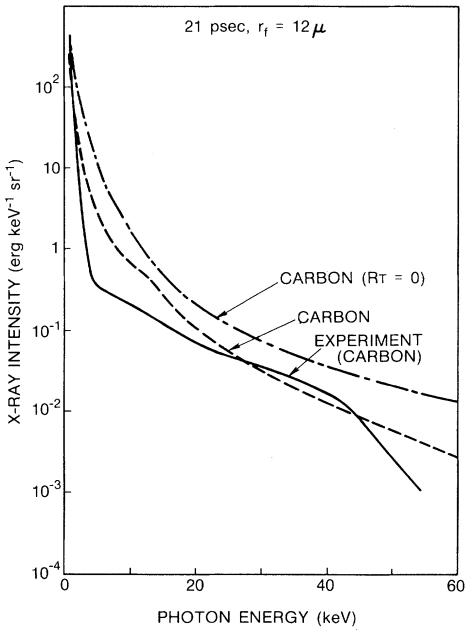

FIG. 4. Time-integrated x-ray emission spectra from Figs. (1) and (2), compared with experiment.

al convenience, the initial conditions contained an exponential-tail density distribution. One might question whether it affects the magnetic-field distribution. After a few picoseconds the laser redistributes the density at the focus, so the only remaining "memory" of the initial conditions is contained in the radial density gradient, $\partial N_e/\partial r$, connecting the redistributed density at the focus with the tail at larger radii. The contribution of this gradient to the magnetic source is indicated by term (2) in Fig. 3. Note that it is everywhere smaller than the other terms.

These conclusions regarding the magnetic-field evolution assist the qualitative understanding of the laser-plasma interaction. They do not, however, directly address experimental measurements. We shall, therefore, present some further analysis on previous experiments, and suggest some new ones.

Measurements of the high-energy tail of the x-ray spectrum are particularly valuable diagnostics because experimentally they are a relatively direct measure of the hot-electron population, whether of suprathermal origin as suggested by some[11] or from spatial regions (where the magnetic field is largest) which have a high thermal temperature, as suggested here. X-ray measurements have proved valuable computationally, because the energetic x-ray spectrum has proved insensitive to computational parameters, such as initial temperature, etc. This is in marked contrast to some other potential diagnostics, such as fast ion emission.

Figure 4 presents the experimental data and the computational results with the basic and complete models. The experiment measured the absolute intensity into 4π sr; and the computational result is also for the absolute intensity, with no adjustable parameters. We can see from Fig. 4 that even though the magnetic-field distributions in the two cases are quite different, the change in the shape of the x-ray spectrum is small. The absolute intensity, however, is brought into quantitative agreement with experiment. The hard x-rays originate from a very small region in space over a very short time and depend very strongly on the electron temperature. For the case with the thermal force included, the peak magnetic field drops by a factor of 3, the maximum electron temperature by a factor of 3 also (19 keV in the case of Fig. 1 versus 60 keV for that of Fig. 2), and the hard x-ray intensity is reduced by a factor of 2. Note that these ratios do not scale as simply as could be expected from a simple analysis because of the complicated geometry involved.

Finally, we remark that the features noted above regarding Fig. 1, particularly items (b), (c), and (d), suggest why there has been some difficulty in reproducing the Faraday rotation measurement of the magnetic field.[2] It appears that such experiments should not use probe beams timed near peak laser intensity and located near the critical depth, but later and much further out.

We would like to thank Dave Bailey of Lawrence Livermore Laboratory and Jess Christiansen of Culham Laboratory who suggested including the effects of the thermal force in laser-target calculations. This work was supported in part by University of Rochester Laboratory for Laser Energetics.

[1]J. A. Stamper *et al.*, Phys. Rev. Lett. 26, 1012 (1971).
[2]J. A. Stamper and B. H. Ripin, Phys. Rev. Lett. 34, 138 (1975).
[3]M. G. Drouet and R. Bolton, Phys. Rev. Lett. 36, 591 (1976).
[4]D. A. Tidman, Phys. Rev. Lett. 35, 1228 (1975).
[5]D. A. Tidman and R. A. Shanny, Phys. Fluids 17, 1207 (1974).
[6]R. S. Craxton and M. G. Haines, Phys. Rev. Lett. 35, 1336 (1975).
[7]J. B. Chase *et al.*, Phys. Fluids 16, 1142 (1973).
[8]D. G. Colombant *et al.*, Phys. Fluids 18, 1687 (1975).
[9]B. H. Ripin *et al.*, Phys. Rev. Lett. 34, 1313 (1975).
[10]S. I. Braginskii, in *Reviews of Plasma Physics*, edited by M. A. Leontovich (Consultants Bureau, New York, 1966), Vol. 1, p. 205.
[11]V. W. Slivinsky, H. N. Kornblum, and H. D. Shay, J. Appl. Phys. 46, 1973 (1975).

Stochastic Acceleration by an Electrostatic Wave near Ion Cyclotron Harmonics*

A. Fukuyama, H. Momota, and R. Itatani
Department of Electronics, Kyoto University, Kyoto, Japan

and

T. Takizuka
Japan Atomic Energy Research Institute, Tokai, Ibaraki, Japan

(Received 6 October 1976)

We study a nonlinear effect on ion motion of an electrostatic wave propagating perpendicularly to a uniform magnetic field. When the wave near the ion cyclotron harmonics has sufficiently large amplitude, the trapped motions of hot ions ($v_\perp > \omega/k_\perp$) become stochastic in the region of appreciable width near the separatrix. Numerical calculations show the tail formation in a $v_\perp$ distribution and theoretically predicted upper bound conditioned by the amplitude.

Formation of a high-energy tail in a velocity distribution of ions has often been observed in experiments on lower-hybrid resonance heating.[1] In order to explain the tail formation, we consider nonlinear motion of an ion affected by a monochromatic electrostatic wave, which has a frequency near an ion cyclotron harmonic and propagates perpendicularly to a uniform magnetic field. For the case of oblique propagation, Smith and Kaufman[2] have recently shown the occurrence of stochastic acceleration along a magnetic field, which is followed by perpendicular acceleration because of energy conservation in the wave frame. However, the threshold of the wave amplitude is so large when $k_\parallel v_{\text{thermal}} \ll \Omega_i$ that their results are not applicable to a lower-hybrid wave. In this Letter, we show that because of the overlapping of islands in a phase plane, irreversible change in magnetic moment can take place even if $k_\parallel$ vanishes and no spatial inhomogeneity exists; this inhomogeneity has been essential for the irreversibility in many analogous studies on cyclotron heating in a mirror field.[3,4]

We consider motion of an ion in a uniform magnetic field $B_0\hat{z}$ in the presence of an electrostatic wave $\varphi\cos(kx-\omega t)$ propagating perpendicularly to the magnetic field. The Hamiltonian of a test ion takes the form,

$$H=[P_x^2+(P_y-m\Omega_i x)^2]/2m + e\varphi\cos(kx-\omega t), \quad (1)$$

where $\Omega_i = eB_0/m$ is the ion cyclotron frequency, and P_x and P_y are the canonical momenta such that $P_x = mv_x$ and $P_y = mv_y + m\Omega_i x$. Since H is independent of y, the momentum P_y is a constant of motion. An appropriate canonical transformation shows that the Hamiltonian may be divided